DOI: 10.61782/fa.2023.1105

forum acusticum 2023

ANALYSIS OF SPECTRA FOR SOUND INSULATION USING METHODS OF MATHEMATICAL STATISTICS AND AI - FIRST APPROACHES

Michael Parzinger[1*] **Ulrich Schanda**[1]

[1] Laboratory for Sound Measurement, Technical University of Applied Sciences Rosenheim, Germany

ABSTRACT

Within the framework of a research focus at the TH Rosenheim on prediction methods for sound and impact sound insulation in timber constructions, methods of mathematical statistics and artificial intelligence are applied to sound insulation. To estimate the potential of those methods, one-third octave band spectra of measured sound insulation of sand-lime brickwork have been analyzed first. On selected data sets for certain building constructions, physically based calculation approaches according to the DIN EN ISO 12354 series of standards, are compared with purely statistical methods such as GAMLSS (Generalized Additive Models for Location, Scale and Shape Parameters). The parameters derived from these procedures can be used for prediction purposes. The interval estimators resulting from these methods are compared. In addition, methods to classify the separating construction based on measurements are discussed. Thereby, in situ, measurements are used in addition to laboratory measurements.

Keywords: *artificial intelligence, mathematical statistics, sound insulation, gamlss*

1. INTRODUCTION

The sound reduction index R is a measure of the frequency-dependent sound insulation of a wall. Physical equations for the sound reduction index depend, among other things, on the separating construction, the loss factor, and the longitudinal wave velocity. DIN EN ISO 12354 [1] provides a variant of the physical sound reduction index. This paper investigates differences between the DIN EN ISO 12354 sound reduction index R and measured laboratory data. For this purpose, the loss factor and the longitudinal wave velocity are fit parameters. So they will be derived from the data. The fitted parameters are then compared with the suggestions from DIN EN ISO 12354. These spectral curves are also compared with spectral curves obtained from a purely statistical method called GAMLSS. In addition, methods to classify the separating construction from measurement data are applied. Finally, further ideas regarding this topic are discussed. These are the estimation of unknown quantities and the contribution to direct and flank transmission of in situ measurements.

**Corresponding author*: *Michael.Parzinger@th-rosenheim.de.*

2. DATA

The in situ measurements of the sound reduction index are just for classifying the construction of the building. All other sections use laboratory data.

2.1 Laboratory data description

The laboratory data used in this paper are from a round-robin test conducted by the Physikalisch-Technische Bundesanstalt (PTB). The data set consists of 24 test bench measurements. In each case, a sand-lime brick [1] wall consisting of equal batches of bricks with a thickness of 24 cm and a mass per unit area of 440 $\frac{\mathrm{kg}}{\mathrm{m}^2}$ was used as the separating construction. [2] and [3] show a detailed description of the laboratory experiments. The wall areas and the respective aspect ratios are also available in the data.

[1] Information on Sand-lime brick: https://www.govinfo.gov/content/pkg/GOVPUB-C13-e0a3f4809397be4cbfeb77507c673889/pdf/GOVPUB-C13-e0a3f4809397be4cbfeb77507c673889.pdf

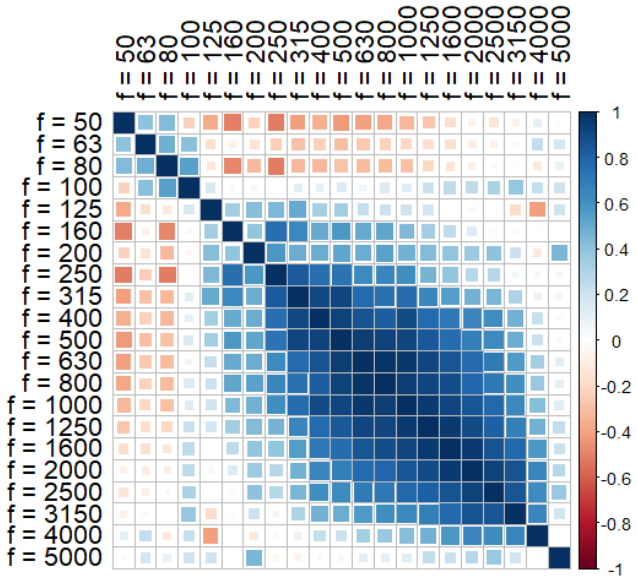

Figure 1: Correlation of the sound reduction index R between different one-third octave bands.

2.2 Laboratory data properties

The data is assumed to follow a normal distribution in each one-third octave band. The Shapiro-Wilk test [4] was used to check the distribution property because this test is suitable for small sample sizes. To avoid the problem of multiple tests, [5] and [6] were considered. Figure 1 shows the correlation of the sound reduction index between the one-third octave bands. The darker or fuller the field, the stronger the correlation. Blue indicates a positive correlation, and red indicates a negative correlation. These correlations are used later for bootstrapping and classification.

2.3 Building measurement data

In addition to laboratory data, 18 data sets with sand-lime bricks from field measurements are available. There are also data sets with other building constructions provided; 16 data sets with brick [2] as construction material and 13 data sets with filling brick. [3] The brick walls have a thickness of 36.5 cm, eleven filling brick walls have a thickness of 24 cm, and the remaining walls have a thickness of 30 cm. Other parameters like aspect ratio or mass per unit area are partly unknown. As before, the assumption of normal distribution has been tested and can be accepted.

[2] Brick information: https://www.gobrick.com/

[3] Filling bricks are bricks with the addition of concrete filling

3. PHYSICAL MODELL

The selected physical model for the sound reduction index R is based on DIN EN ISO 12354. Accordingly, $R = -10\lg(\tau) - 10\lg\left(1 + \frac{c_0 S_{\text{tot}}}{8Vf}\right)$ with transmission factor

$$\tilde{\tau} = \begin{cases} \frac{Z_0^2}{(m'\pi f)^2}\left(\frac{\pi}{2}\frac{\sigma^2}{\eta_{\text{tot}}}\frac{f_c}{f} + \frac{2\sigma_f}{(1-f^2/f_c^2)^2}\right), & f < 0.89 f_c \\ \frac{Z_0^2}{(m'\pi f)^2}\frac{\pi}{2}\frac{\sigma^2}{\eta_{\text{tot}}}, & 0.89 f_c \leq f \leq 1.4 f_c \\ \frac{Z_0^2}{(m'\pi f)^2}\frac{\pi}{2}\frac{\sigma^2}{\eta_{\text{tot}}}\frac{f_{c,\text{eff}}}{f}, & f > 1.4 f_c \end{cases}$$

$\tau = \max(\tilde{\tau}, \tau_{\text{plateau}})$ and $\tau_{\text{plateau}} = \left(\frac{4\rho_0 c_0}{1.1\rho c_{\text{L}}}\right)^2 \frac{1}{50\eta_{\text{tot}}}$.

Where $f_c = \frac{\sqrt{3}c_0^2}{\pi c_{\text{L}} t}$ is the critical frequency, $f_{c,\text{eff}} = (4.05\frac{tf}{c_{\text{L}}} + \sqrt{1 + (4.05\frac{tf}{c_{\text{L}}})^2})$ is the effective critical frequency, and $\eta_{\text{tot}} = \eta_{\text{int}} + \frac{\text{C}}{\sqrt{f}}$ is the total loss factor. Here $\frac{\text{C}}{\sqrt{f}}$ describes the boundary loss. The radiation coefficient σ and the radiation coefficient for forced waves σ_f are implemented according to DIN EN ISO 12354, where σ is limited to 1.18 and σ_f to two. Table 1 shows all other occurring characteristics. Please note that the wall thickness of 25 cm in Table 1 includes the plaster layer, while the otherwise mentioned thickness of 24 cm ignores the plaster layer.

4. PARAMETER ESTIMATION

4.1 Fit parameters

The goal is to estimate the longitudinal wave velocity c_{L}, the internal loss factor η_{int}, and the constant C from the data. Therefore, c_{L}, η_{int}, and C will be referred to as fit parameters. Let $\theta = (\eta_{\text{int}}, \text{C}, c_{\text{L}})$ and $R(f|\eta_{\text{int}}, \text{C}, c_{\text{L}}) \equiv R(f|\theta)$ be the previously defined physical sound reduction index R at frequency f with parameter vector θ. Also, let $y_{if} \in \mathbb{R}_{\geq 0}$ be the measured laboratory sound reduction index R of the i-th wall at frequency f, where $i = 1, \ldots, 24$ and $f \in \{50, 63, \ldots, 4000, 5000\}$.

The values for θ are obtained by solving the optimization problem in equation (1), which is equivalent to minimizing the squared distance between the physical model and the measured data.

Table 1: Characteristics for the sound reduction index R.

Symbol	Description	Value
c_0	Sound speed in air	340 m/s
S_{tot}	Total surface in reception room	85 m²
V	Reception room volume	50 m³
Z_0	Sound characteristic impedance of air	400 $\frac{Pa}{m/s}$
m'	Mass per unit area	440 kg/m²
t	Construction thickness	0.25 m
c_{L}	Longitudinal velocity	Fit parameter
C	Constant	Fit parameter
η_{int}	Internal loss factor	Fit parameter
ρ_0	Density of air	$\frac{400}{340}$ kg/m³
ρ	Density of the material	1760 kg/m³

$$\hat{\theta} := \underset{\theta \in \mathbb{R}^3_{\geq 0}}{\arg\min} \sum_{i=1}^{24} \sum_{f} (y_{if} - R(f|\theta))^2 \tag{1}$$

$$\hat{\theta}_\eta := \underset{(\text{C}, c_{\text{L}}) \in \mathbb{R}^2_{\geq 0}}{\arg\min} \sum_{i=1}^{24} \sum_{f} (y_{if} - R(f|\text{C}, c_{\text{L}}))^2 \tag{2}$$

$$\hat{\theta}_{\text{C}} := \underset{(\eta_{\text{int}}, c_{\text{L}}) \in \mathbb{R}^2_{\geq 0}}{\arg\min} \sum_{i=1}^{24} \sum_{f} (y_{if} - R(f|\eta_{\text{int}}, c_{\text{L}}))^2 \tag{3}$$

If $R(f|\text{C}, c_{\text{L}}) := R(f|\eta_{\text{int}} = 1\%, \text{C}, c_{\text{L}})$ and $R(f|\eta_{\text{int}}, c_{\text{L}}) := R(f|\eta_{\text{int}}, \text{C} = 440/485, c_{\text{L}})$, then equations (2) and (3) are the optimization problems when the internal loss factor η_{int} and C get a fixed value. Table 2 and DIN EN ISO 12354 show the corresponding values. For the longitudinal wave velocity c_{L}, DIN EN ISO 12354 only gives the value for the material and not for a sand-lime brick wall. For this reason, optimization with fixed longitudinal wave velocity is not performed.

The equations were solved using the programming language R [7]. Therefore, the R package *minpack.lm* [8], which uses the Levenberg-Marquardt algorithm, has been applied.

4.2 Estimation results

Figure 2 compares the sound reduction index of a 24 cm thick sand-lime brick wall between the values from DIN EN ISO 12354 Table B.2 and the values after estimating the three fit parameters from the data. Especially for low and high frequencies, there is a big difference between the DIN EN ISO 12354 values and the measured data. The sound reduction index, whose fit parameters are derived by equation (1) is relatively close to the mean value of the data.

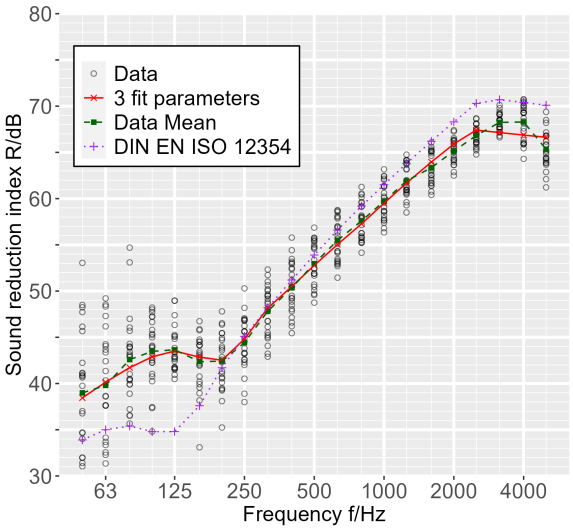

Figure 2: Comparison between the sound reduction index of measured values (data), data mean, values according to DIN EN ISO 12354 Table B.2, and the spectral curve fit with three fit parameters.

Figure 3 shows the different spectral shapes of the sound reduction index depending on whether all three fit parameters or only two of them are estimated. The spectral curve according to DIN EN ISO 12354 is omitted for clarity.

To better compare these spectra, statistical distance measures are needed. These measures indicate the distance between the measured data and the models. One possibility is the RMSE (root-mean-square error) according to equation (4). Note that the factor $\frac{1}{24 \cdot 21}$ is obtained from the 24 buildings and 21 one-third octave bands. The RMSE shows the root of the mean squared distance between the data and the model.

$$\text{RMSE} = \sqrt{\frac{1}{24 \cdot 21} \sum_{i=1}^{24} \sum_{f} (y_{if} - R(f|\theta))^2} \tag{4}$$

The RMSE has the disadvantage that it depends strongly on the standard deviation of the data. Therefore,

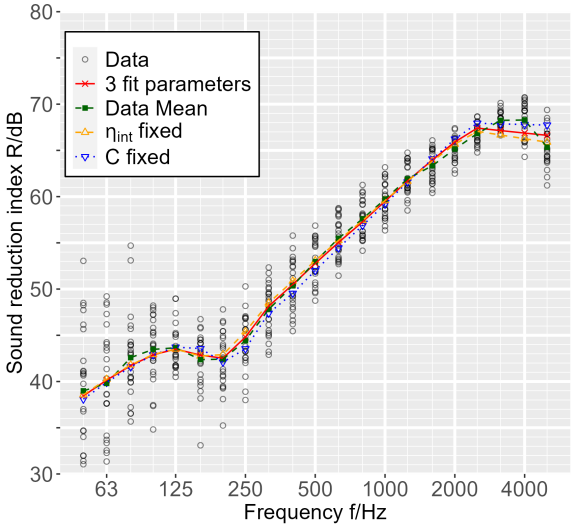

Figure 3: Comparison between the sound reduction index of measurements (data), data mean, the spectral curve fitting with three fit parameters, the spectral curve fitting where η_{int} is fixed, and the spectral curve fitting where C is fixed.

the normalized root mean squared error, or NRMSE, is considered. Equation (5) defines the NRMSE at frequency f, where $\bar{y}_f := \frac{1}{24}\sum_{i=1}^{24} y_{if}$. For the NRMSE, at a frequency, the RMSE between the data and a model is divided by the RMSE between the data and the data mean. In the best case, $\text{NRMSE}_f = 1$ holds; then the model R passes through the mean $\bar{y}_f$ at frequency f. The value $\text{NRMSE}_f = 1 + a$ with $a > 0$ would mean that at frequency f, the RMSE of this model is $100 \cdot a\%$ higher than for a model that passes through the mean.

$$\text{NRMSE}_f = \sqrt{\frac{\sum_{i=1}^{24}(y_{if} - R(f|\theta))^2}{\sum_{i=1}^{24}(y_{if} - \bar{y}_f)^2}} \tag{5}$$

The averaged NRMSE_f according to equation (6) can be used to compare the models. The interpretation is then similar to before the RMSE of the model is $100 \cdot (\text{NRMSE} - 1)\%$ higher on average than the RMSE of a model that would pass through the data mean.

$$\text{NRMSE} = \frac{1}{21}\sum_{f} \text{NRMSE}_f \tag{6}$$

Figure 4 shows the NRMSE comparison for each frequency between DIN EN ISO 12354 Table B.2 and the estimation with three fit parameters. The NRMSE of the fitted model is closer to one for each frequency. So the fitted model describes the data for each frequency better than the model according to DIN EN ISO 12354.

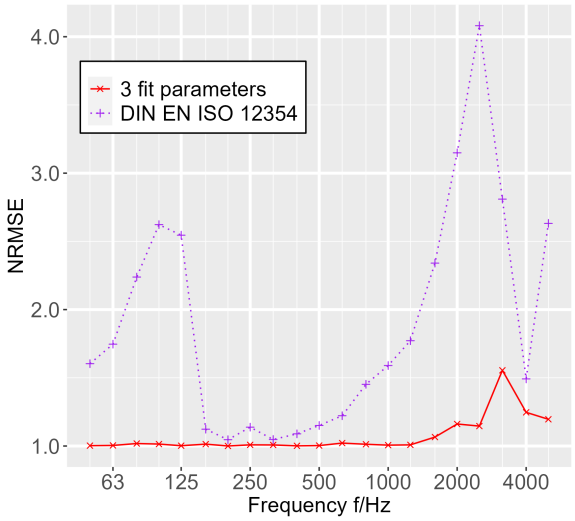

Figure 4: Comparison between the NRMSE of values according to DIN EN ISO 12354 Table B.2 and the spectral curve fit with three fit parameters.

Figure 5 shows the NRMSE between the three-parameter fit and the two-parameter fits. Of these three models, the model with three fit parameters describes the data best; however, in the frequency range above 2000 Hz, the physical model improperly describes the sound reduction of thick plates and the associated other waveforms not accounted for in the model.

Table 2 shows the results of the estimates. While the DIN EN ISO 12354 gives the internal loss factor for sand-lime brick as 0.01, the data estimate it to be 0.03; keeping the constant C fixed, the estimated internal loss factor is 0.07. The constant C is $\frac{m'}{485}$ according to the DIN EN ISO 12354, where m' is the mass per unit area. In our case, $m' = 440$ kg/m² holds, therefore $\frac{m'}{485} \approx 0.91$. The estimated values for C are 2.13 and 2.68, respectively. The estimated longitudinal wave velocity values lie around 1000 m/s instead of 2500 m/s.

4.3 Interval Estimations

Previously, point estimates were applied. Now parametric bootstrapping [9] derives interval estimates. Parametric bootstrapping generates random vectors to estimate the fit

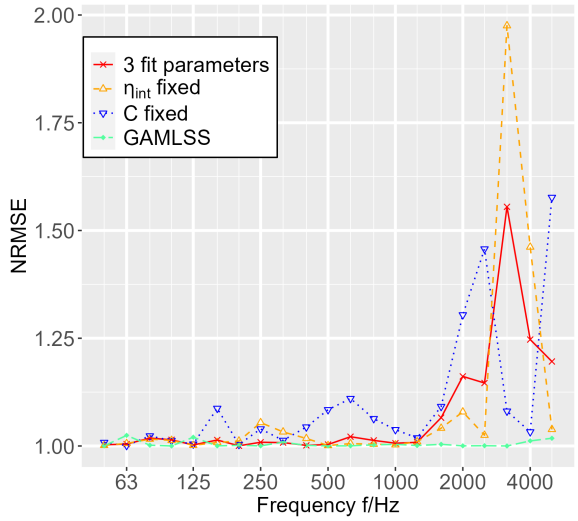

Figure 5: Comparison between the NRMSE of the fit with three fit parameters, the fit with fixed η_{int}, the fit with fixed C, and GAMLSS.

Table 2: Estimated fit parameter. Values in **bold** were estimated from the data.

Unit	η_{int}	C	c_{L} m/s	RMSE dB	NRMSE
Norm	0.01	0.91	2500	5.27	1.86
3 par.	**0.03**	**2.13**	**1046**	3.11	1.07
η_{int}, fixed	0.01	**2.68**	**1061**	3.13	1.09
C, fixed	**0.07**	0.91	**978**	3.17	1.10

parameters and repeats this process an arbitrary number of times. The random vectors must have similar statistical properties as the data.

In our case, random vectors are generated with a 21-dimensional normal distribution with mean vector μ and covariance matrix Σ, in short, $\mathcal{N}_{21}(\mu, \Sigma)$. The expectation vector $\mu \in \mathbb{R}^{21}$ contains the 21 means at the different frequencies, and $\Sigma \in \mathbb{R}^{21\times 21}$ contains both the frequency-dependent variances on the diagonal and the covariance between two different frequencies. Random sampling generates 24 of these vectors to simulate 24 new walls. This simulation of new measurement data is then repeated B times to generate B possible fit parameters. In our case, B = 1000 holds.

Table 3 shows the results of parametric bootstrapping. Here, 95 % of the fit parameters lie between the 2.5 % and 97.5 % quantiles, and 50 % lie between the 25 % and 75 % quantiles. Also, other quantities can be derived with bootstrapping. For example, the estimated correlation between the internal loss factor and C is -0.8. This correlation is plausible since the internal loss factor and C are used to calculate the total loss factor. The correlation of the remaining parameters will not be discussed further, as it is only weak.

Table 3: Parameter distribution after bootstrapping.

Unit	η_{int}	C	c_{L} m/s
2.5-%-quantile	0.014	1.47	1001
25-% quantile	0.024	1.88	1030
Median	0.029	2.12	1043
Mean	0.028	2.15	1043
75-% quantile	0.033	2.39	1056
97.5-% quantile	0.041	2.97	1083

A nonparametric bootstrapping variant yielded almost identical results.

5. GAMLSS

GAMLSS is short for Generalized Additive Model for Location, Scale, and Shape. GAMLSS is a nonlinear and semiparametric method and does not take the physical model as a basis sound reduction index R. Instead, GAMLSS estimates a function from the data. This estimated function is composed piecewise of polynomials [10].

Figure 6 compares the spectral curve of a GAMLSS with the spectral curve from the physical with three fit parameters. Figure 5 shows that GAMLSS provides the best result. However, GAMLSS does not result in a physical interpretation.

6. BUILDING MATERIAL CLASSIFICATION

This section uses the laboratory data set from subsection 2.1 and the building data set from subsection 2.3. Four separate constructions are available to calculate the sound reduction index R. These are sand-lime brick, filling brick, brick from the building measurements, and the previously used laboratory sand-lime brick data. The goal is to detect the separating components with the help of the sound reduction index. For this purpose, the classification methods will be presented in the following three subsec-

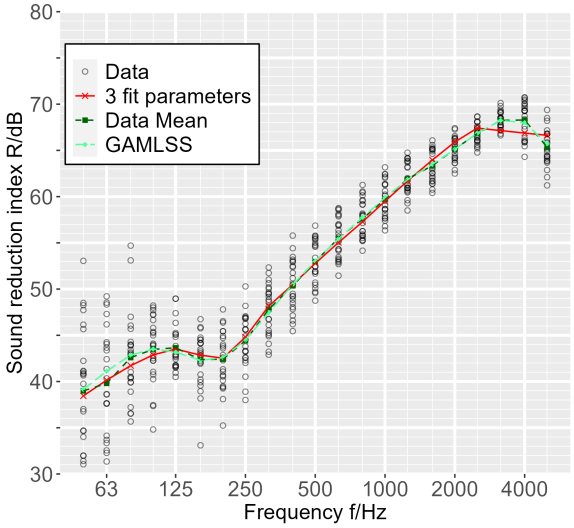

Figure 6: Comparison between the sound reduction index of measurements (data), data mean, the spectral curve fit with three fit parameters and GAMLSS.

tions to discuss the results in subsection 6.4. Also, let C_j be the j-th construction in this section with $j = 1, \ldots, 4$.

6.1 Naive Bayes Classifier (NBC)

The Naive Bayes Classifier is a simple approach based on probability density functions. The goal is to find the construction C_j that maximizes the probability density of C_j given the measured R values. The R or R' value at a frequency f is noted as r_f, then $\arg\max_j p(C_j|r_{50}, \ldots, r_{5000})$ is to be found. With Bayes' theorem $p(C_j|r_{50}, \ldots, r_{5000}) \propto p(C_j)p(r_{50}, \ldots, r_{5000}|C_j)$ holds, thereby $\propto$ specifies that this equation is true except for negligible constants. The Naive Bayes Classifier assumes that the measurements for each frequency and each construction are independent. Then $p(r_{50}, \ldots, r_{5000}|C_j) = \prod_f p(r_f|C_j)$ is true for each j. Note that this assumption is not appropriate here because of the correlations shown in Figure 1, but for this reason, the label naive is justified. $p(C_j)$ defines the prior probability often used in Bayesian statistics. Assuming each construction is equally likely $p(C_j)$ can be ignored. Overall, the Naive Bayes classifier searches for the C_j that maximizes the expression $\prod_f p(r_f|C_j)$, where $p(r_f|C_j)$ is the probability density function of a normal distribution at the frequency f of the construction C_j.

6.2 Quadratic Discriminant Analysis (QDA)

The Naive Bayes Classifier assumes that the measurements between frequencies are independent. Figure 1 shows that the measurements are not independent due to their correlation. Quadratic Discriminant Analysis takes the covariance structure into account. Otherwise, this procedure works like the Naive Bayes Classifier, i.e., a new sound reduction index spectral curve $r \in \mathbb{R}^{21}$ is classified to maximize the expression in equation (7).

$$l(r|C_j) = -\log|\Sigma_j| - (r - \mu_j)'\Sigma_j^{-1}(r - \mu_j) \qquad (7)$$

$\mu_j \in \mathbb{R}^{21}$ and $\Sigma_j \in \mathbb{R}^{21\times 21}$ denote the expectation vector and covariance matrix of construction C_j, respectively. The means of the corresponding measurements are the estimations of μ_j. The covariance matrices Σ_j must be inverted in (7), but the estimation with the Pearson method are poorly conditioned and numerically problematic to invert, see [11] page 100-104. Instead, the estimation with the Ledoit-Wolf linear shrinkage estimator [12] is used. The idea of the Ledoit-Wolf linear shrinkage estimator is to find the optimal convex linear combination of the sample covariance matrix and the identity matrix. For further information about QDA, see [13].

6.3 Support Vector Machine (SVM)

Support Vector Machine for binary classification creates a hyperplane that separates the two classes as much as possible. In the case of more than two classes, each class is tested against every other class, which is a so-called one-against-one classification. The hyperplane is transformed with a kernel function to learn non-linear relationships. See [14] to find more details about Support Vector Machine. The R package *e1071* [15] provides a function to apply SVM. The argument *type* was set to "nu-classification" while the rest was left as default.

6.4 Classification results

This subsection discusses the results of classification using the previously presented methods. Table 4 shows the results when only in situ measurements were used, and Table 5 shows the results using laboratory measurements. In these tables, SL stands for building sand-lime bricks, FB for filling bricks, B for bricks, and SLL for the laboratory sand-lime brick measurements. The methods Naive Bayes Classifier, Quadratic Discriminant Analysis, and Support Vector Machine are abbreviated as NBC, QDA, and SVM, respectively. The Acc column shows the relative number

Table 4: Classification results: In situ measurements.

			True			Acc
	Method		SL	FB	B	
Prediction	NBC	SL	14	3	0	0.83
		FB	4	9	0	
		B	0	1	16	
	QDA	SL	17	3	0	0.89
		FB	1	9	0	
		B	0	1	16	
	SVM	SL	17	3	0	0.89
		FB	1	9	0	
		B	0	1	16	

Table 5: Classification results: In situ and laboratory measurements.

			True				Acc
	Method		SL	FB	B	SLL	
Prediction	NBC	SL	10	2	0	3	0.76
		FB	4	8	0	1	
		B	0	1	16	0	
		SLL	4	2	0	20	
	QDA	SL	15	2	0	1	0.87
		FB	0	8	0	0	
		B	0	1	16	0	
		SLL	3	2	0	23	
	SVM	SL	14	4	0	2	0.82
		FB	0	7	0	1	
		B	0	1	16	0	
		SLL	4	1	0	21	

of correct classifications. The SL column of Table 4 can then be read as follows: according to the Naive Bayes Classifier method, sand-lime brick was correctly identified as such 14 times and incorrectly classified as filling brick four times. The FB column shows that filling brick was correctly identified by NBC nine times, classified as sand-lime brick three times, brick once, and so on. The values themselves were derived with leave-one-out cross-validation (LOOCV). LOOCV means that for all methods, all but one of the measured spectral curves were used to train the models and then to classify the construction of the omitted measured spectral curves.

Overall, the results show that it is possible to classify the construction based on the measurement spectral curves. Especially with Quadratic Discriminant Analysis, which showed an accuracy of 89 % for the construction measurements and an accuracy of 87 % when laboratory measurements were taken into account.

It is important to note that due to the data situation, it is not clear whether the results are so promising because the construction was recognized so well, or whether other construction properties caused different spectral curves and these were recognized. It should be noted that parameters such as the mass per unit area are unknown for the construction measurements. To exclude that the methods discriminate between the mass per unit area or other parameters instead of the construction, more data or a physical model for the building sound reduction index R' is needed to estimate the missing parameters.

7. CONCLUSION AND FUTURE WORK

The results show that the estimated loss factor and the longitudinal wave velocity do not agree with DIN EN ISO 12354-1 values. While DIN EN ISO 12354-1 assumes an internal loss factor of 1%, C $= \frac{m'}{485}$, and a longitudinal wave velocity of $c_\mathrm{L} = 2500$ m/s, the estimated values lie by approximately $\eta_\mathrm{int} = 3\%$, C $= \frac{m'}{207}$, and $c_\mathrm{L} = 1050$ m/s. The NRMSE value of 1.07 for the model with estimated values is much lower than the NRMSE of 1.86 for the model with DIN values. A perfect value would be an NRMSE of one, which means that the model runs through the mean of the data. Wall area and side ratios were considered in the calculations, but they have a minor influence on the sound reduction index.

To validate the estimated values, other models for the physical sound reduction index R should be investigated in the future, in addition to the model according to DIN EN ISO 12354. The DIN EN ISO 12354 itself refers to the work of [16], [17], and [18].

Naive Bayes Classifier, Quadratic Discriminant Analysis, and Support Vector Machine methods classified the separating construction. Quadratic Discriminant Analysis gives excellent results, with an accuracy of 89 % on the building measurements and an accuracy of 87 % when laboratory measurements are also taken into account.

Verifying whether the classification is based on the component or on other factors is difficult. Therefore, in the future, methods will be used to estimate unknown quantities such as mass per unit area from the data. In addition, it should be possible to distinguish between the contribution of direct and flanking transmission of in situ measurements.

8. ACKNOWLEDGMENTS

Thanks to Physikalisch-Technische Bundesanstalt for the laboratory data of sand-lime brick walls from the round-robin test and to Müller-BBM and ifbSorge for data from in situ measurements.

9. REFERENCES

[1] DIN EN ISO 12354-1:2017-11, "Bauakustik – Berechnung der akustischen Eigenschaften von Gebäuden aus den Bauteileigenschaften: Teil 1: Luftschalldämmung zwischen Räumen."

[2] W. Weise and V. Wittstock, "Using round robin test results for the accreditation of laboratories in the field of building acoustics in germany," *Building Acoustics*, no. 12, pp. 189–206, 2005.

[3] DIN EN ISO 10140-5:2021-09, "Akustik - Messung der Schalldämmung von Bauteilen im Prüfstand - Teil 5: Anforderungen an Prüfstände und Prüfeinrichtungen (ISO 10140-5:2021); Deutsche Fassung EN ISO 10140-5:2021."

[4] S. S. SHAPIRO and M. B. WILK, "An analysis of variance test for normality (complete samples)," *Biometrika*, vol. 52, no. 3-4, pp. 591–611, 1965.

[5] C. E. Bonferroni, *Teoria statistica delle classi e calcolo delle probabilità*. Pubblicazioni del R. Istituto superiore di scienze economiche e commerciali di Firenze, Seeber, 1936.

[6] Sture Holm, "A simple sequentially rejective multiple test procedure," *Scandinavian journal of statistics, theory and applications*, vol. 6, no. 2, pp. 65–70, 1979.

[7] R Core Team, *R: A Language and Environment for Statistical Computing*. R Foundation for Statistical Computing, Vienna, Austria, 2023.

[8] T. V. Elzhov, K. M. Mullen, A.-N. Spiess, and B. Bolker, *minpack.lm: R Interface to the Levenberg-Marquardt Nonlinear Least-Squares Algorithm Found in MINPACK, Plus Support for Bounds*, 2022. R package version 1.2-2.

[9] B. Efron, "Bootstrap methods: Another look at the jackknife," *Annals of statistics*, vol. 7, no. 1, 1979.

[10] R. A. Rigby and D. M. Stasinopoulos, "Generalized additive models for location, scale and shape,(with discussion)," *Applied Statistics*, vol. 54, pp. 507–554, 2005.

[11] D. A. Belsley, E. Kuh, and R. E. Welsch, *Regression diagnostics: Identifying influential data and sources of collinearity*. Wiley series in probability and mathematical statistics, New York: John Wiley & Sons, 1980.

[12] O. Ledoit and M. Wolf, "A well-conditioned estimator for large-dimensional covariance matrices," *Journal of multivariate analysis*, vol. 88, no. 2, pp. 365–411, 2004.

[13] Venables W. N. and Ripley B. D., *Statistical Analysis of Financial Data in S-Plus*. New York: Springer-Verlag, 2004.

[14] C. Cortes and V. Vapnik, "Support-vector networks," *Machine learning*, vol. 20, no. 3, pp. 273–297, 1995.

[15] D. Meyer, E. Dimitriadou, K. Hornik, A. Weingessel, and F. Leisch, *e1071: Misc Functions of the Department of Statistics, Probability Theory Group (Formerly: E1071), TU Wien*, 2023. R package version 1.7-13.

[16] R. A. Novak, "Radiation from partially excited plates," *Acta Acustica united with Acustica*, vol. Band: 3 ; Seiten: 560-567, 1995.

[17] J. L. Davy, "Predicting the sound insulation of single leaf walls: extension of cremer's model," *The Journal of the Acoustical Society of America*, vol. 126, no. 4, pp. 1871–1877, 2009.

[18] C. Hopkins, *Sound Insulation*. Butterworth-Heinemann, 2007.